ALPHA FOUNDATION FOR THE IMPROVEMENT OF MINE SAFETY AND HEALTH

Final Technical Report

Project Title	Refining silica and other dust particle classification by optical light microscopy
Grant Number	AFC316FO-84
Organization	Virginia Polytechnic Institute and State University
Principal Investigator	Emily Sarver
Contact Information	Email: esarver@vt.edu Phone: 540-231-8139 Fax: 540-231-4070
Period of Performance:	Sept 1, 2021 – Aug 31, 2023

Acknowledgement/Disclaimer: This study was sponsored by the Alpha Foundation for the Improvement of Mine Safety and Health, Inc. (ALPHA FOUNDATION). The views, opinions and recommendations expressed herein are solely those of the authors and do not imply any endorsement by the ALPHA FOUNDATION, its directors and staff.

1 Executive Summary

Current technologies for monitoring coal mine dust do not provide real-time information about dust composition. For example, the continuous personal dust monitor (CPDM) reports dust mass concentration but not dust constituents; rather, to determine constituents, sample filters must be collected and analyzed post-hoc. Thanks to recent improvements in image processing and portable microscopy, solutions that were previously confined to the laboratory can now be used for near real-time field monitoring. In a previous project, we showed that optical microscopy with automated image processing could effectively distinguish between respirable sized coal and mineral particles—enabling a binary classification of dust. In the current work, we explored the possibility of expanding this approach to subclassify minerals, including silica. The work proceeded under three main tasks, as follows.

Task 1: Build a dust image library. To characterize optical features associated with different particle types, a library of images was compiled using dust generated from four sources: high purity silica (quartz) and kaolinite powders were used to represent common silicates in coal mine dust; and a real clean coal material and real a rock dust product (i.e., high purity limestone) were used to represent the coal and rock dust constituents in coal mine dust. The images were used collect data on individual particles of different sizes and present under different levels of loading density within the image frame. An important precursor to this work was developing a sequential sampling and imaging method, and particle tracking algorithm, such that individual particles could be identified based on their material source. An image library was first built for respirable dust particles; and later the library was expanded to include somewhat larger particles (i.e., about 10-20 μm) as explained below. In all, images were capture for 1,148 unique sample frames (i.e., fields of view), which included a total of 97,729 particles.

Task 2: Explore particle features to support classification modelling. Using the respirable dust particle image library, it was determined that accurate silica classification was probably not feasible—regardless of limits on particle size or loading density within a frame. However, a model was developed for classifying particles into three classes (coal, silicates, and carbonates), which could enable respirable dust source apportionment in many mines. The model relies on pairs of images collected in plane- and cross-polarized light, and requires only one feature to classify particles (i.e., the mean greyscale intensity measured in both images).

Notably, we initially expected that both particle size and loading density would impact accuracy of classification based on optical features. However, results using respirable sized dust suggested that loading density, within the practical range for imaging (i.e., where individual can be distinguished), is probably not important. On the other hand, particle size might be very important, with an increase in particle size showing increased potential for separation between silica and kaolinite. Indeed, this observation led us to expand the project work under Task 1 to image somewhat larger particles. Then, we were also able to expand the Task 2 to explore features that might be exploited for silica classification. Results indicated that using a combination of particle greyscale intensity and texture features might be favorable.

Task 3: Validate classification model. Work under this task was limited to respirable size particles due to the project timeline. To challenge the respirable dust source apportionment model, new samples were generated using the same clean coal and rock dust product as used previously; but instead of high purity silica and kaolinite—which might not be widely representative of silicates in coal mine dust—real roof rock materials from several mines were used. When using the model to apportion dust into three classes (coal, silicates, carbonates), results showed that the difference between the model predictions and actual portions for each class was less than 8% (by particle count).

Three main accomplishments from this project should be highlighted: (1) In the respirable size range, a model has been developed for classification of particles (as coal, silicate, or carbonate) based only on their optical intensity in plane- and cross-polarized light image pairs. Envisioning a portable microscopy application where dust is deposited and imaged frequently, this could enable a real-time monitor for coal mine dust source apportionment in many operations. (2) While a simple method for silica classification using portable microscopy appears unlikely in the respirable size range, results for somewhat larger particles more promising, especially if both optical intensity and texture features are considered. Given that dust in the 10-20 µm range might still serve as a useful proxy for respirable dust in terms of composition, continued research focused on silica classification in this range appears prudent. (3) For exploration of particle features and development of classification models, reference measurements are critical—and identification of each particle *a priori* can optimally serve as an direct reference measurement. This is simple for images collected on dust samples with a single, high purity particle source; but the problem is quite complex for composite samples, which are necessary for interrogating the effects of particle interactions and testing model accuracy. Here, an innovative method was devised involving sequential sampling (dust deposition) and imaging events, with particle tracking between events. This approach could be used or adapted for other applications in the future.

2 Problem Statement and Objective

Exposure to respirable coal mine dust (RCDM) can cause lung diseases such as pneumoconiosis, progressive massive fibrosis, and chronic obstructive pulmonary disease [1]–[3]. Ongoing or resurgent prevalence of occupational lung disease among coal miners in the US and elsewhere has underscored the importance of effective RCMD monitoring strategies [4]. Acknowledging the role of crystalline silica in many cases, a 2018 consensus report published by the National Academies of Sciences, Engineering, and Medicine called for development of real-time silica monitoring capabilities; it also called for an overall better understanding of dust sources, and development and/or application of technologies to enable broad monitoring of RCMD trends [4].

At present, real-time RCMD monitoring technologies only measure mass and particle concentrations, but not individual constituents. Indeed, there are only two types of devices currently certified as intrinsically safe for use in US coal mines: The continuous personal dust monitor (CPDM, such as the PDM3700; Thermo Fisher Scientific, Waltham, Massachusetts) is mandated for regulatory compliance monitoring (per 30 CFR part 74), and measures mass concentration of respirable dust using a tapered element oscillating microbalance. A device called the personal DataRAM (pDR-1000; Thermo Fisher Scientific, Waltham, Massachusetts) is also permissible—though it has been recently discontinued by the manufacturer—and measures particle concentration in the respirable range using a light scattering technique [5]. Despite significant interest, real-time monitoring of specific RCMD constituents like crystalline silica has not yet come to fruition. Beyond the considerable costs of research and development, and sort of niche context of coal mining environments, there is also the challenge of analytical sensitivity. For example, silica might only represent a small percentage of the total RCMD mass, which itself is relatively small. However, a viable alternative to monitoring specific constituents of RCMD could be to track larger components, which are often correlated.

A prior proof-of-concept project, also funded by the Foundation (AFC316FO-74), envisioned a field-microscopy based monitoring solution (e.g., as shown in Figure 2.1). That research showed respirable-sized dust particles could be classified as either coal or minerals using just a pair of images [6]. To elaborate, after collecting dust particles onto a glass sampling substrate, static images were collected in both plane-polarized (PP) and cross-polarized (CP) light. The PP image was used to identify all particles in the image frame; and the CP image was used to identify mineral particles in the frame, since they typically illuminate based on their birefringence. Supposing samples can be collected and imaged on a semi-continuous basis, the approach could support a simple binary classification of RCMD (i.e., mineral versus coal). This could be valuable on its own in certain applications, like tracking the relative dust generation from mining rock strata versus the target coal seam at the production face [6]. Moreover, in an environment where silica content is understood to correlate well with the overall mineral component of RCMD, even a crude measurement of that component might be valuable if made frequently.

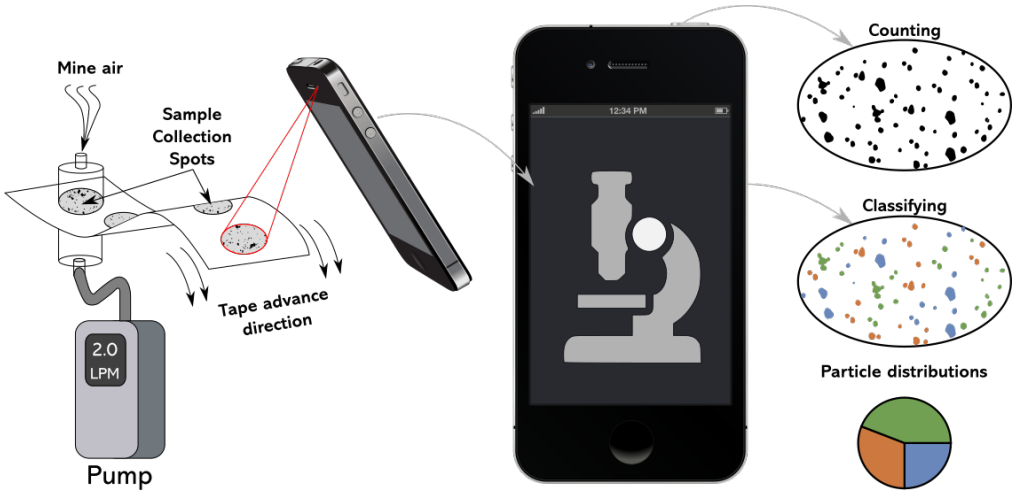

Figure 2.1. Conceptual illustration of coal mine dust monitor that uses a "cell-phone" microscope to count and classify particles.

Nevertheless, an obvious improvement in microscopy-based particle classification would be the capability to distinguish between different mineral components, including silica. For this, our previous results suggested that two factors may be critical: particle size and particle loading density (PLD) in the image frame. Regarding size, finer particles are more difficult to classify since the display of optical properties is limited by the microscope resolution. Thus, size—measured here as projected area diameter (PAD)—is inversely proportional to particle classification accuracy. Regarding PLD, this factor may affect the influence on particles on each other. For instance, particles that ordinarily have limited brightness (greyscale or color "intensity") may appear brighter when in close proximity to other bright particles in an image frame.

To further the optical microscopy dust monitoring concept, the ultimate aim of the current project was to refine a mineral sub-classification model, including for silica, which incorporates any necessary criteria to deal with particle size and loading density limits. Work was split into three primary tasks: (1) building a particle image inventory; (2) exploring particle features to enable classification modeling; and (3) validation of the modeling.

3 Research Approach

3.1 Task 1: Dust Image Inventory

3.1.1 Dust Materials

In many coal mines, the primary components of dust can be loosely associated with three primary sources: Coal is sourced from the target coal seam itself; silicate minerals such as aluminosilicates and silica are frequently sourced from the rock strata surrounding the coal seam; and carbonate minerals such as calcite are frequently sourced from inert 'rock dust' products (generally high purity limestone) that are applied to mitigate explosion risks [7]–[10]. While other constituents can be present in RCMD, such as metal sulfides or oxides, they typically do not account for a substantial portion of mass or particle count [9], [11]. Thus, for the current project we used four source materials to generate dust particles for imaging, feature analysis and model development: (1) a clean bituminous coal product (obtained from an industry partner) was used to represent coal; (2) MIN-U-SIL 5 or MIN-U-SIL 10 (US Silica, Katy, TX, USA), which are high-purity quartz powders were used as the source of silica particles, and (3) a high-purity kaolinite powder (Ward's Science, Rochester, NY, USA) was used to represent other silicates; and a real limestone rock dust product (obtained from an industry partner) was used as a representative source of carbonates. While the silica, kaolinite and rock dust were obtained as powders, the coal required milling to enable respirable-sized particles to be sampled. It was pulverized and sieved to obtain -230 mesh material as the source of coal dust.

For model testing (see section 3.3), the same coal and rock dust material were again used as dust sources. However, to better represent the range of silicate minerals that might occur in RCMD (i.e., beyond pure silica and kaolinite) and determine if the optical characteristics of the silicates in real materials were comparable, three real rock strata materials were obtained from industry partners. The two materials designated as "ROM rock" represent the rock strata that was mined at the production face in two different mines (Mine 11 and Mine 14); these were pulled from the run-of-mine (ROM) material on the production belt and were pulverized and sieved prior to sampling of respirable-sized particles. The material designated as "bolter dust" was obtained directly from the dust collection system on a roof bolter machine at Mine 16. This material was already fine and required no preparation prior to respirable sampling.

To determine the purity of the seven materials used in this work, respirable-sized particles of each material were analyzed by scanning electron microscopy with energy dispersive X-ray (SEM-EDX). Briefly, a sample of each material was collected in the lab using a $10-mm$ nylon cyclone at 2.0 L/min to discard over-sized particles. The dust was collected on 37-mm polycarbonate (PC) filters in closed styrene cassettes. A 9-mm subsection of each filter was cut and prepared for analysis by sputter coating with Au/Pd. Then, the computer-controlled SEM-EDX routine described by Sarver et al. (2021) [9] was used to identify, size and collect elemental data on about 500 particles per sample in the 1-10 µm range. Per Sarver et al. (2021) [9], particles were classified using their elemental content, and the mass percentage in each class was estimated using particle dimensions and assumed values for specific gravity. The SEM-EDX work was conducted using an FEI Quanta 600 FEG environmental scanning electron microscope

(ESEM) (Hillsboro, OR, USA). This microscope was equipped with a backscatter electron detector (BSD) and a Bruker Quantax 400 EDX spectroscope (Ewing, NJ, USA). The following parameters were used for SEM-EDX analysis routines: 1000x magnification, 12.5 working distance, 15 kV accelerating voltage, and a spot size of 5.5 µm. The resulting mass distribution of particles is shown in Table 3.1. The carbonaceous class is generally interpreted as coal particles; silicates include silica, aluminosilicates and other silicates; and the carbonates include calcium and magnesium carbonates.

Table 3.1. SEM-EDX characterization of respirable dust composition for each source material (C=coal, S=silicates, CB=carbonates)

Material	mass %			
	C	S	CB	Others
Silica	1.06	98.93	0.00	0.00
Kaolinite	0.00	100.00	0.00	0.00
Rock dust	4.10	0.57	95.32	0.19
Coal	99.91	0.09	0.00	0.09
ROM rock (mine 14)	9.85	84.76	0.19	5.20
ROM rock (mine 11)	5.62	93.60	0.00	0.78
Bolter dust (mine 16)	9.20	89.40	0.20	1.20

3.1.2 Sampling Design

To assess the behavior of the optical properties of each particle type when present with other particle types, all samples were prepared as composites. Since silica was of the most interest for this project, the sampling was designed such that composites always contained silica plus one other particle type (i.e., kaolinite, rock dust or coal). As explained in the next section, we used a sequential sampling design whereby silica was first deposited on the sample slide, and then the other particle type was deposited.

Because this project explored the effects of PAD and PLD on classification accuracy, it was important to collect data on a large number of image frames (i.e., there is one PLD value per frame) and a large number of particles (i.e., there is one PAD value per particle). Since we used a standard enclosure and a similar quantity of bulk feed material for each dust sampling event, the deposition time (i.e., the run time of the sampling pump) was effectively used to control PLD. On the other hand, PAD was controlled by the source materials and the sampling size collectors. For respirable dust sampling, we used a 10-mm nylon cyclone at a flow rate of 2.0 L/min, which yields a top size of about 10 µm. Later, we also experimented with a different sampling apparatus to enable capture of somewhat larger particles (i.e., between about 10-20 µm); this is described in more detail in section 3.4.

3.1.3 Dust collection and imaging

Dust sampling on the previous project was conducted such that, for each sampled collected on a glass substrate for optical microscope imaging, a replicate sample was collected on an

adjacent polycarbonate filter for reference measurements by SEM-EDX. However, this sort of reference measurement has inherent uncertainty since (a) the measurement is done on a replicate sample rather than the same sample being used for the optical microscopy, and (b) the SEM-EDX method itself may not be completely accurate (e.g., some coal particles could be misclassified as mineral particles). Thus, for the current project, we devised a new method for sampling which enables direct reference measurements.

Briefly, particles from a single source are deposited in sequence onto a transparent, non-birefringent, sticky surface and images are captured following each deposition event on the same frames (i.e., fields of view). The sticky surface is an acrylic double-sided tape (Maxwell Manufacturing, Hangzhou, China). It minimizes particle movement between deposition and imaging, such that individual particles can be tracked in the sequence of images. Figure 3.1 shows the comparison of a glass slide and a double-sided tape under both plane-polarized (PP) and cross-polarized light (CP). The double-sided tape does not show signs of birefringence or light polarization in any particular direction, meaning it should not interfere with the basic premise for particle classification (i.e., to exploit differences in the birefringence or other optical features of different particle types).

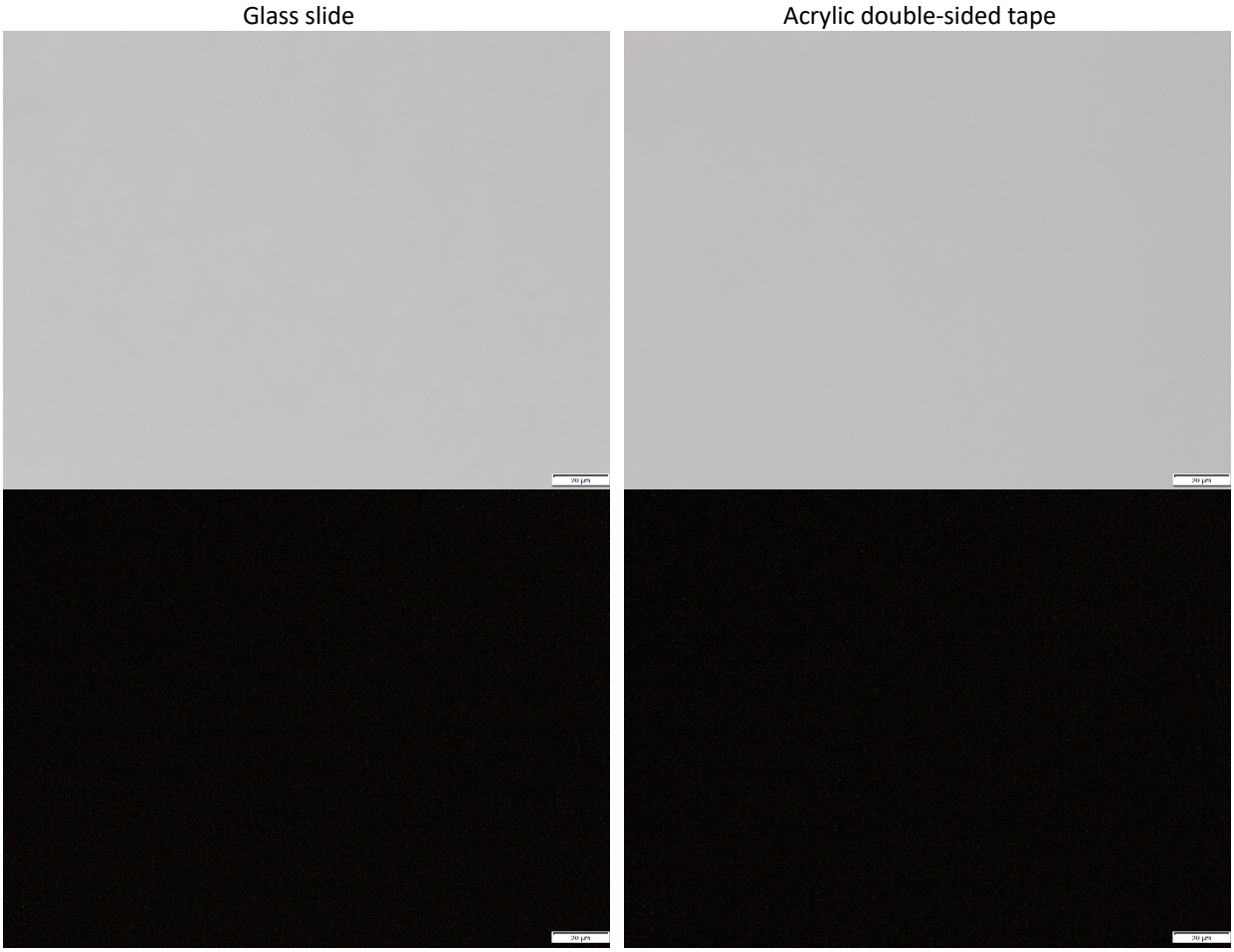

Figure 3.1. OM images of a glass slide (left) and acrylic double-sided tape (right) under PP light (top) and CP light (bottom).

Figure 3.2 shows a summary of the sample preparation method for two sampling stages. To begin, the double-sided tape is cut and mounted to a 22mm x 22 mm glass slide, and the slide is placed inside a filter cassette for dust loading. After the first type of particles (e.g., silica) has been deposited, the glass slide is removed from the cassette and fixed in a 3D-printed slide holder; the holder was printed to maintain an x-y reference point for the microscope stage, such that we can revisit the same frames for each imaging event. After capturing OM images under desired lighting conditions (i.e., plane and cross polarized light in reflected and/or transmitted mode), the glass slide is moved back to the cassette, and the next particle type is loaded (e.g., kaolinite). Then, the slide is placed back into the special holder for imaging again. This process can be repeated until all the desired particle types have been deposited and imaged (i.e., any number of stages).

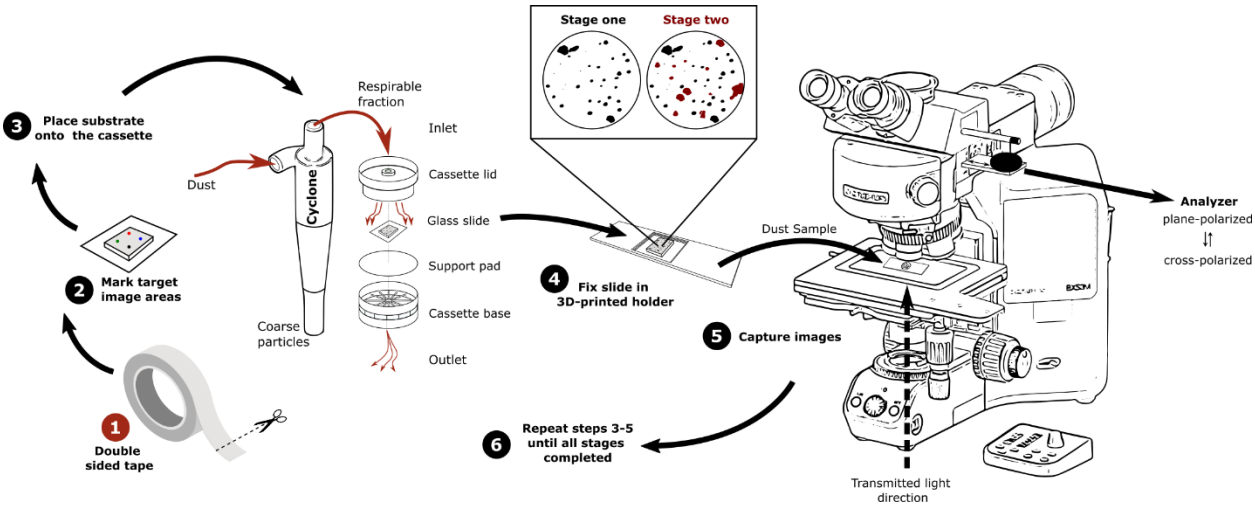

Figure 3.2. Dust collection and imaging procedure.

3.1.4 Particle identification

The major benefit of the sequential dust collection and imaging procedure shown in Figure 3.2 is that—so long as particles stay in place once deposited—it allows for individual particle tracking. And if high-purity materials are used to generate the different dust particle types, this means the identity of each particle can be assigned with high confidence.

A particle tracking algorithm was developed to automatically find and identify particle types based on images with sequential deposition of known particle types. Figure 3.3 shows an overview of the method used to track particles. First, all particle pixels are determined in a PP image containing multiple particle types deposited sequentially (e.g., silica + kaolinite), and a default class is assigned to the particles. After the particle's x and y coordinates and circularity[1] are extracted, the process is repeated on the previous PP image(s) containing one less particle type (e.g., only silica). The algorithm tries to match each particle in the second image (e.g., only silica) with the most similar particle in the first image (e.g., silica + kaolinite) by minimizing the Euclidean distance between particles in the feature space. If the minimum distance does not

[1] x, y, and circularity were chosen as features for particle tracking working under the assumption that the particle location and shape should not dramatically change between sequential dust collection.

reach a certain threshold (determined by trial and error to maximize accurate classification), the default classification is applied. In the case of a sample with silica + kaolinite, particles that match between two sequential images are classified as silica, and those that only show up in the multiple-particle type image are classified as kaolinite.

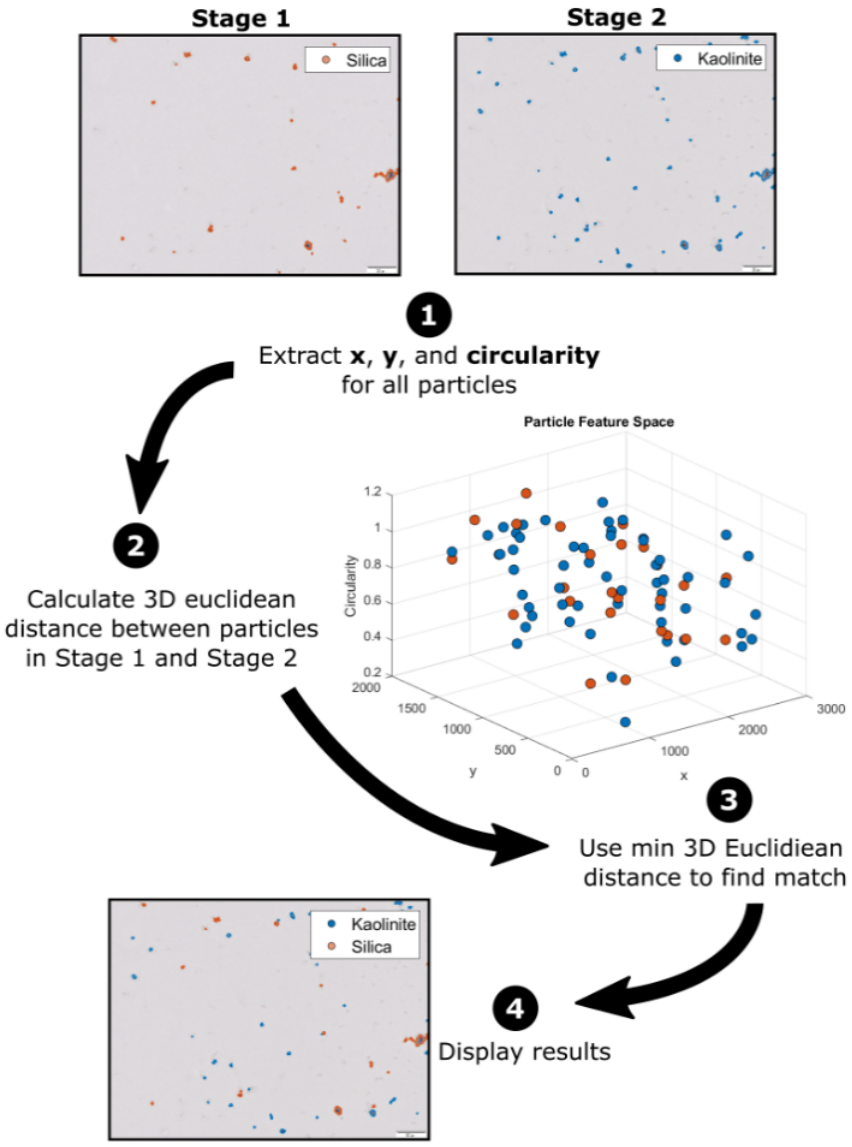

Figure 3.3. particle tracking methodology.

Figure 3.4 shows examples of particle tracking achieved by comparing images of a given sample frame following each dust deposition event. (It is noted that very fine particles are not included in the particle tracking. Per the previous project, extraction of optical features from these particles is challenged by the OM resolution; and we have observed here that they are more likely to be displaced between loading events.) These examples clearly illustrate how the

identification of new particles in each image in a sequence can be used as a direct measurement of the particles of a specific type deposited in the immediately preceding loading event.

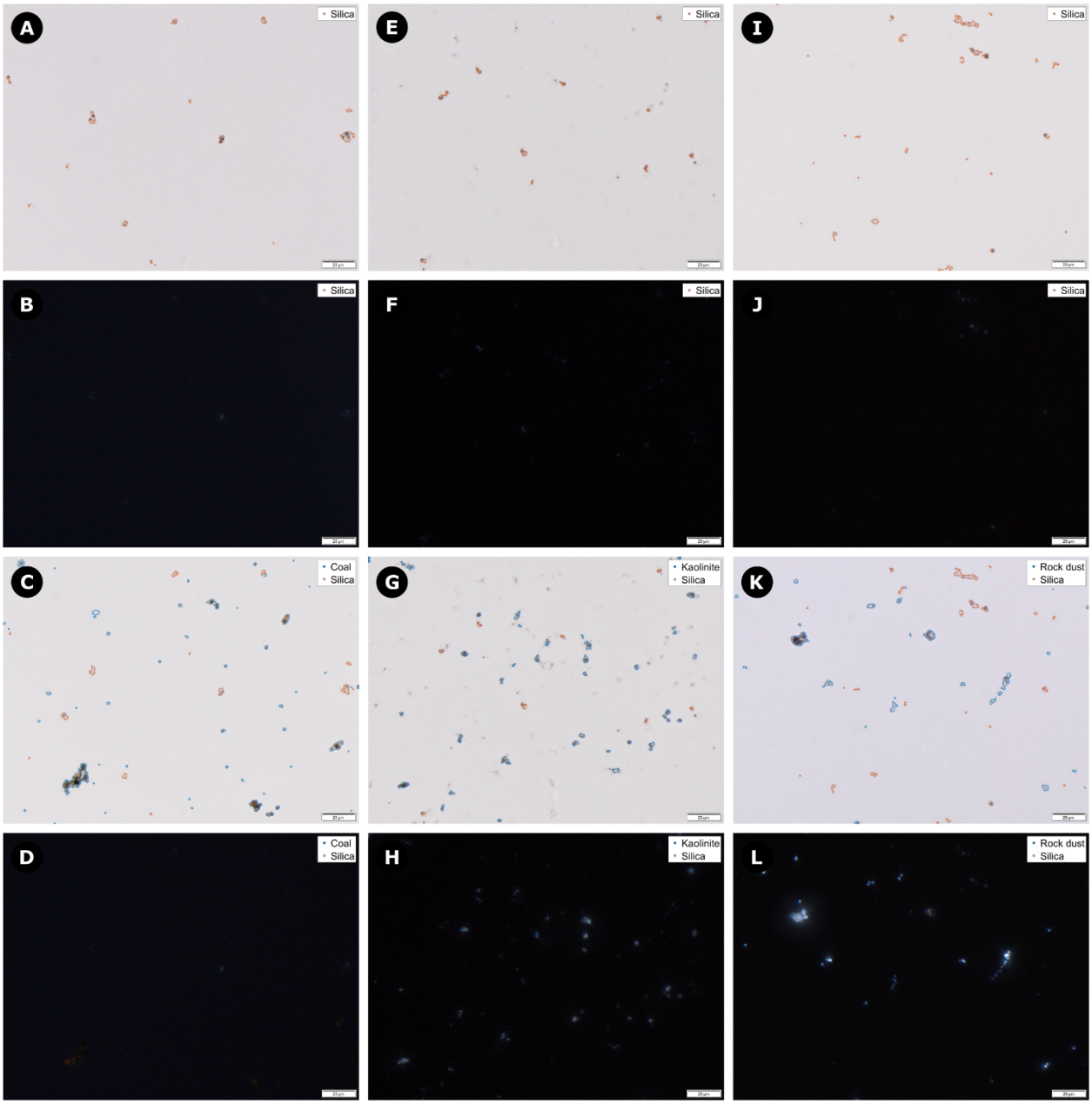

Figure 3.4. Stage-one TPP images (top row) of three dust samples that were loaded with respirable sized silica (A, E, and I), followed by their TCP pairs (B, F, and J). Stage-two TPP images (preceding the bottom row) show respirable sized coal (C), kaolinite (G), or rock dust (K) particles, followed by their TCP pairs (D, H, and L). On TPP images, the particle boundaries have been determined for silica (orange), coal, kaolinite, and rock dust (blue) to show automated particle tracking between dust-loading events.

3.1.5 Image inventory

For respirable particles, Table 3.2 summarizes of the total number of frames imaged and the total number of silica and other particles for each sample type (i.e., as determined by the

particle tracking algorithm). As mentioned, some preliminary work was also done to image and explore the optical features of somewhat larger particles, and that work is described in section 3.4.

Table 3.2. Dust image inventory for respirable size particles.

Material	Sample Frames	Particles
Silica	93	667
Kaolinite		1769
Silica	37	101
Coal		1947
Silica	45	319
Rock dust		508
Total	**175**	**5311**

3.2 Task 2: Exploration of particle features

3.2.1 Effect of PLD and PAD on respirable size particle features

The sample frames/particles shown in Table 3.2 were used to develop a particle classification model for respirable sized particles. For each particle, the tracking algorithm was used to assign its "true" class (i.e., silica, kaolinite, rock dust or coal), and other features were also attached including: its measured PAD in the PP image; the PLD for the PP image it was captured in; and its greyscale intensity in both the PP and CP images.

Particle classification was primarily based on two particle intensity features: The aggregated mean particle intensity (AMPI) computes the sum of the mean greyscale intensity of a given particle between the images in PP and CP light. The multiplication of the mean grayscale intensities (MMPI) instead multiplies the particle's intensity between the two images. The AMPI and MMPI values were computed during particle feature extraction.

Figure 3.5 shows the values of AMPI and MMPI as PLD and PAD increase. The solid lines indicate the average values of AMPI or MMPI for the particles in a specific class, while the shaded area in different colors represents the standard deviation. The x-axis represents the minimum PAD or PLD allowed in the dataset for calculating the mean and standard deviation. In other words, only particles with values greater than or equal to the specified value are included at each x-position.

The results illustrate that, as expected, particle classification may be improved as PAD increases. However, somewhat unexpectedly, the influence of PLD is less pronounced. However, there is a particular point where PLD becomes so high that individual particles can no longer be discerned in the image. As PLD does not appear to affect particle characteristics (at least within the range where individual particles are still distinguishable by the particle tracking algorithm), subsequent analysis did not consider the influence of PLD.

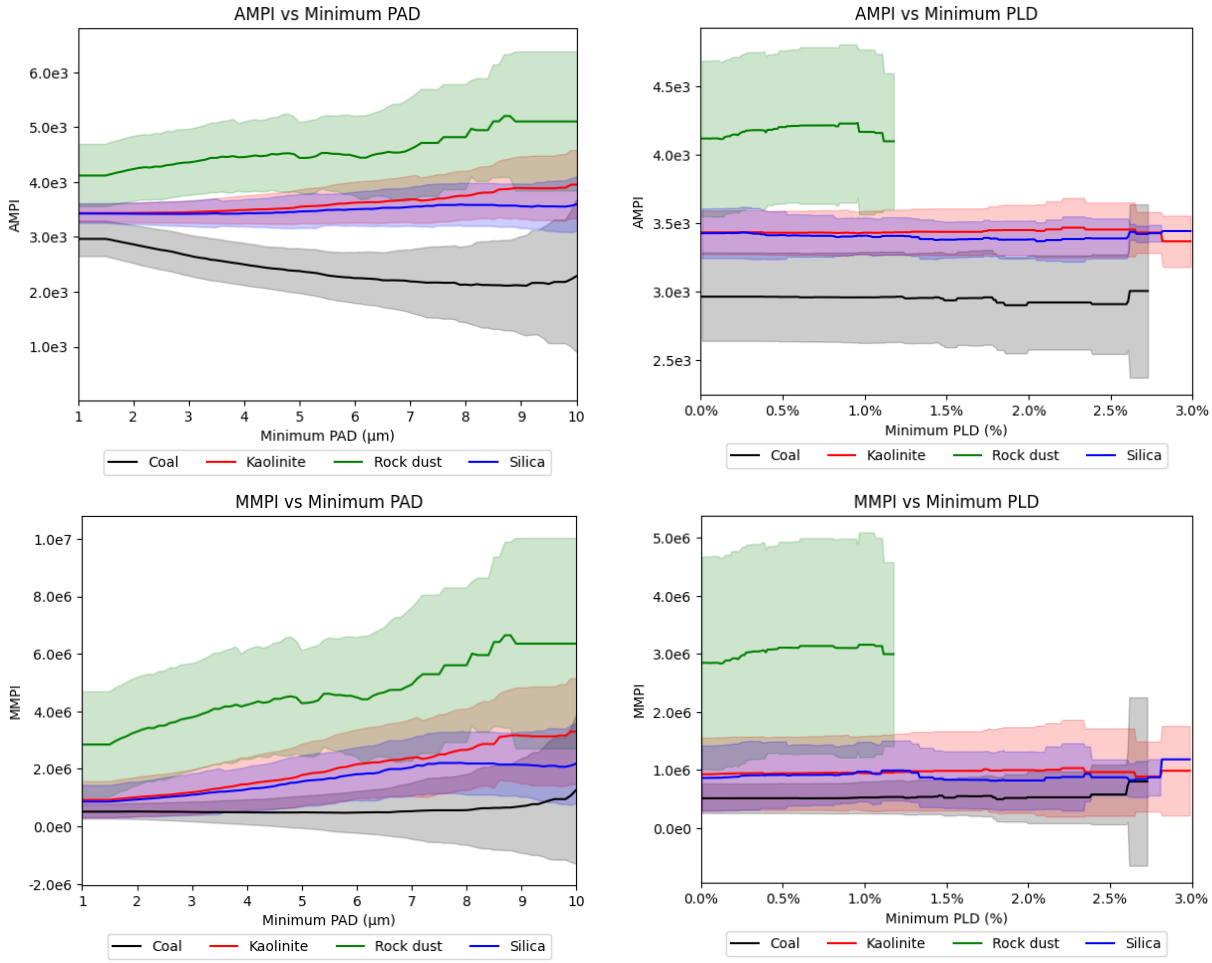

Figure 3.5. AMPI (top) and MMPI (bottom) values for respirable sized particles as a function of PAD (left) and PLD (right).

To explore the effect of PAD on particle classification, particles were split into "low" and "high" PAD bins using the median (50th percentile) as a threshold which was around 2.5 µm. Figure 3.6 presents the distribution of AMPI and MMPI values, respectively, for all particles in the respirable dust image inventory binned into the low or high PAD. For silica, Figure 3.5 and Figure 3.6 show there is significant overlap with kaolinite across most of respirable range. Nevertheless, the results suggest that it should be possible to use AMPI and MMPI to classify particles into three major fractions: coal, silica + kaolinite, and carbonates. This is important because, if the silica + kaolinite class holds for a broader range of silicate minerals, such a classification scheme could be helpful for tracking the primary dust sources in coal mines.

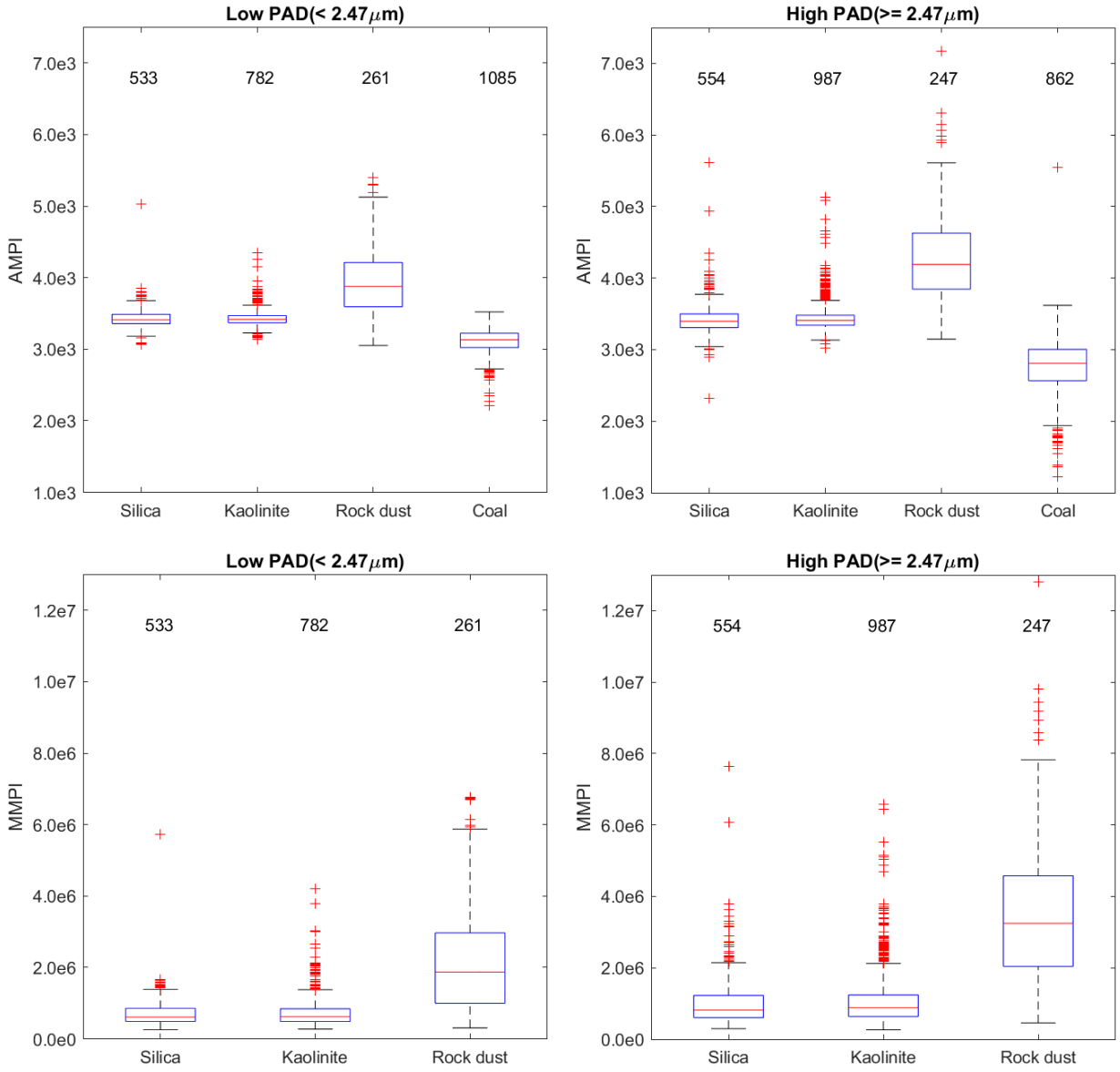

Figure 3.6. Distribution of AMPI (top) and MMPI (bottom) values for respirable sized particles with low (left) or high PAD (right).

3.2.2 Coal/silicates/carbonates classification model

Recognizing the value of a source apportionment tool, a coal/silicates/carbonates classification model was built from the respirable dust image inventory (i.e., particles included in Table 3.2) using a two-step approach: first, an AMPI threshold was used to separate coal particles from total minerals; then, an MMPI threshold was applied to the total minerals to separate silicates from carbonates. Figure 3.7 shows the specific AMPI and MMPI thresholds, which were determined to minimize the differences between precision and recall across all three classes.

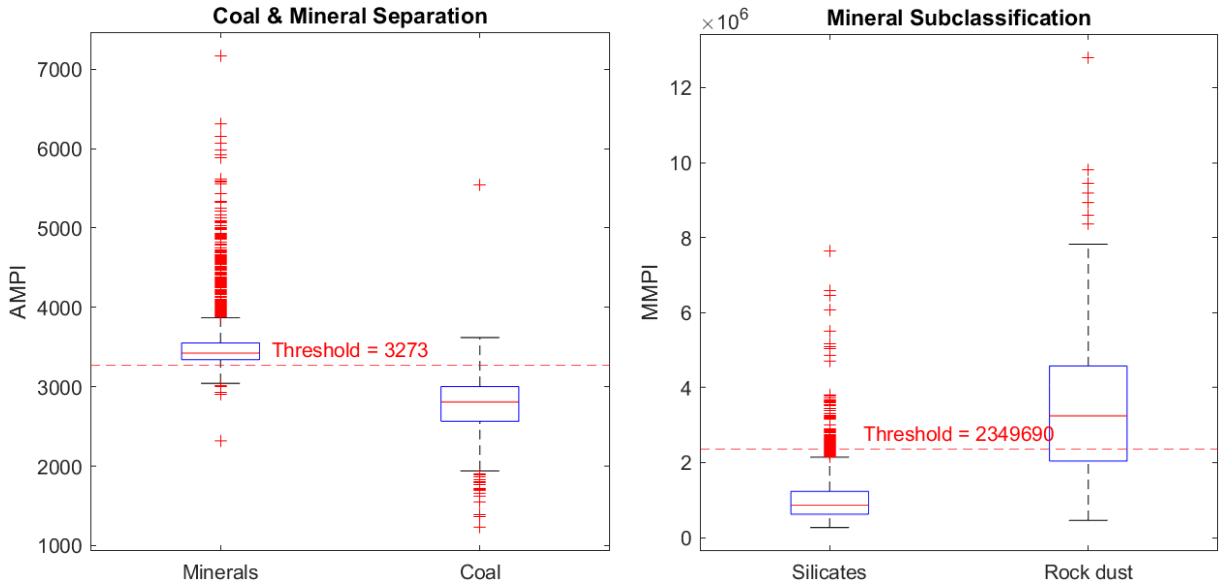

Figure 3.7. Distribution of AMPI (left) and MMPI (right) values for respirable size particles. The AMPI and MMPI thresholds indicated on the plots were determined to be optimal for the coal/silicates/carbonates model.

Precision is defined as the ratio between true positives to all positive predictions made by the model (Equation 1). For example, suppose the model predicts the class of 100 particles as coal, but only 80 of those particles are actually coal while the other 20 are either silicates or carbonates. In this scenario, the number of true positives is 80 (items the model predicted as coal that were actually coal), and the number of false positives is 20 (items that the model predicted as coal but were actually silicates and carbonates). The precision in this case would be 80/(80+10+10) = 0.8.

$$Precision = \frac{True\ Positives}{True\ Positives + False\ Positives} \qquad \text{(Equation 1)}$$

Recall is the ratio of true positive predictions to all actual positive instances in the dataset (Equation 2). For example, suppose the model predicts the class of 300 coal particles as follows: 220 coal particles, 30 silicate particles, 50 carbonate particles. In this scenario, the number of true positives is 220 (items the model predicted as coal that were actually coal), and the number of false negatives is 80 (items that were actually coal but the model predicted as either silicates or carbonates). The recall in this case would be 220/(220+30+50) = 0.73.

$$Recall = \frac{True\ Positives}{True\ Positives + False\ Negatives} \qquad \text{(Equation 2)}$$

Precision and recall are often in tension with each other. Increasing precision typically reduces recall and vice versa. This trade-off is inherent in many classification problems, and the choice

between optimizing for precision or recall depends on the specific problem and its requirements. For this work, we balanced the two metrics to assess the overall model performance. To achieve balance, we evaluated precision and recall values for each of the three classes. This resulted in a total of six values which were then used to calculate the standard deviation. Since our aim was to find a balance between precision and recall, a high standard deviation indicates greater difference between the values, while a low standard deviation indicates a better balance.

We used a simple algorithm to find the combination of AMPI and MMPI thresholds which yielded the minimum standard deviation (11.22%). Using these thresholds, the classification model had a 13.5% misclassification rate for particles included in the respirable dust image inventory (Table 3.2). As illustrated in Figure 3.8, much of the misclassification is due to overlap between the silicates and carbonates classes. In essence, some rock dust particles had relatively low MMPI values whereas some silica and kaolinite particles had relatively high values.

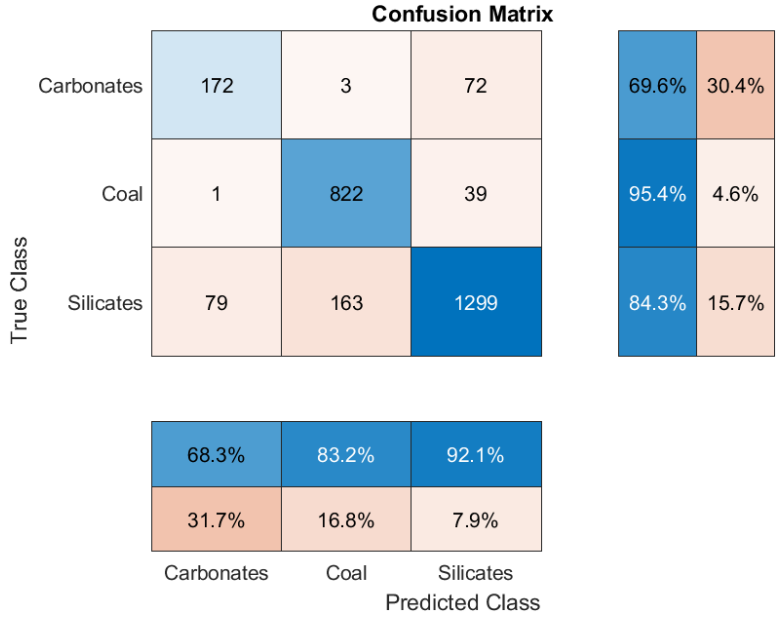

Figure 3.8. Confusion matrix displaying the overall count of observations in regards to true and predicted classes for the coal/silicates/carbonates model for respirable size particles.

3.3 Task 3: Validate classification model

The coal/silicates/carbonates model for respirable size particles was challenged with additional samples. Although the model was developed using particles generated from real coal and rock dust materials, the silica and kaolinite particles used might not widely represent the silicates typical of real rock strata encountered in coal mines. To test the performance of the model on dust particles generated from real rock strata, three materials obtained from industry partners were used. These included two samples of raw rock material that was handpicked from the run-of-mine production belt in Mines 11 and 14, and one sample of material taken directly from the roof bolter dust collection box in Mine 16. The data in Table 3.1 confirms that the respirable size particles from these materials was primarily silicates.

Using the same sequential sampling and imaging approach described above, model validation samples were generated as shown in Table 3.3. For these samples, the rock strata particles (Mine 11, 14 or 16 sources) were deposited first, followed by either coal or rock dust particles (using the same source materials as for the model development samples). The particle tracking and identification methodology was again applied to assign a true class to each particle in an imaged frame, and to extract the particle's feature data.

Table 3.3. Mine materials used for validation of the coal/silicates/carbonates model for respirable dust.

Material	Sample Frames	Particles
ROM rock mine 11	31	651
Rock dust		251
ROM rock mine 11	16	131
Coal		1176
Bolter dust mine 14	32	345
Rock dust		503
Bolter dust mine 14	28	17
Coal		535
ROM rock mine 16	31	920
Rock dust		434
ROM rock mine 16	15	87
Coal		99
Total	**153**	**5149**

When the coal/silicates/carbonates model was applied to the validation samples, the difference between the predicted and actual classes was no more than 15% (Figure 3.9). On average, the percentage difference across all results in Figure 3.9 was 4.4%. Across all particle classes, the average error was 4.4% for coal, 5.3% for silicates, and 3.3% for carbonates. The maximum observed difference was for the Mine 14 ROM + coal sample, where the model underpredicted the coal % and overpredicted the silicates %. This might be due to impurities in the coal particles, though the same effect was not observed for the Mine 11 ROM + coal sample, which had similar proportions of coal and rock strata particles. On the other hand, for the Mine 16 BD + coal sample, the model somewhat overpredicted coal % and underpredicted silicates %. This could be due to inherent coal content in the bolter dust material used as the silicates source for this sample. The small carbonate % predicted in this sample could also be due to relatively bright silicate particles in the bolter dust material. Notably, the discrepancy between silicates and carbonates in the validation samples is quite low.

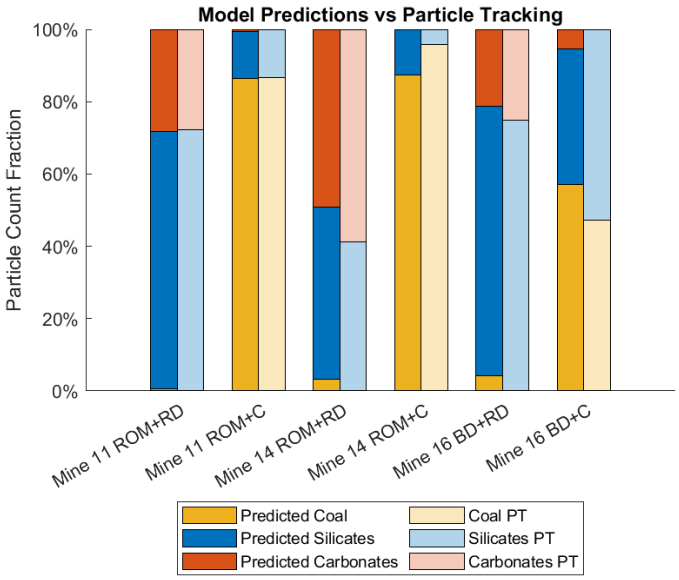

Figure 3.9. Validation results for the coal/silicates/carbonates classification model using respirable size dust particles. Darker bars to the left in each comparisonrepresent the results of the classification model, whle lighter bars represent the results obtained by the particle tracking (PT) approach to assign a "true" identity to each particle.

3.4 Preliminary Work on Larger Particles

While classification of silica, specifically, was not feasible in the respirable size range, a close inspection of Figure 3.5 suggests this might be possible if somewhat larger particles are considered. (For that matter, the coal/silicates/carbonates model might also be improved with increasing PAD.) And, since the compositional distribution of particles in the 10-20 µm range might still be representative of the respirable range (e.g., see [12]), we decided it was prudent to expand the work on this project to include a preliminary analysis of somewhat larger particles. The following sections describe this work.

3.4.1 Modified sampling system

To sample somewhat larger particles, we replaced the respirable dust cyclone with a series of two impactors that were obtained from AerosolWorks LLC (Figure 3.10). The impactors were designed based on the recommendations in [13] to accommodate the same pump flow rate used for respirable dust sampling (i.e., 2.0 L/min using the ELF pump). The impactors were also designed to hold a microscope slide with the sticky surface that served as the impaction plate, and to allowed easy access to retrieve samples between imaging stages (Figure 3.11). In theory, particles >40 µm (aerodynamic diameter) should be deposited on the first plate, with most of the finer particle bypass it. Then, the 10-40 µm particles should deposit on the second plate, with most of the finer particles bypassing it.

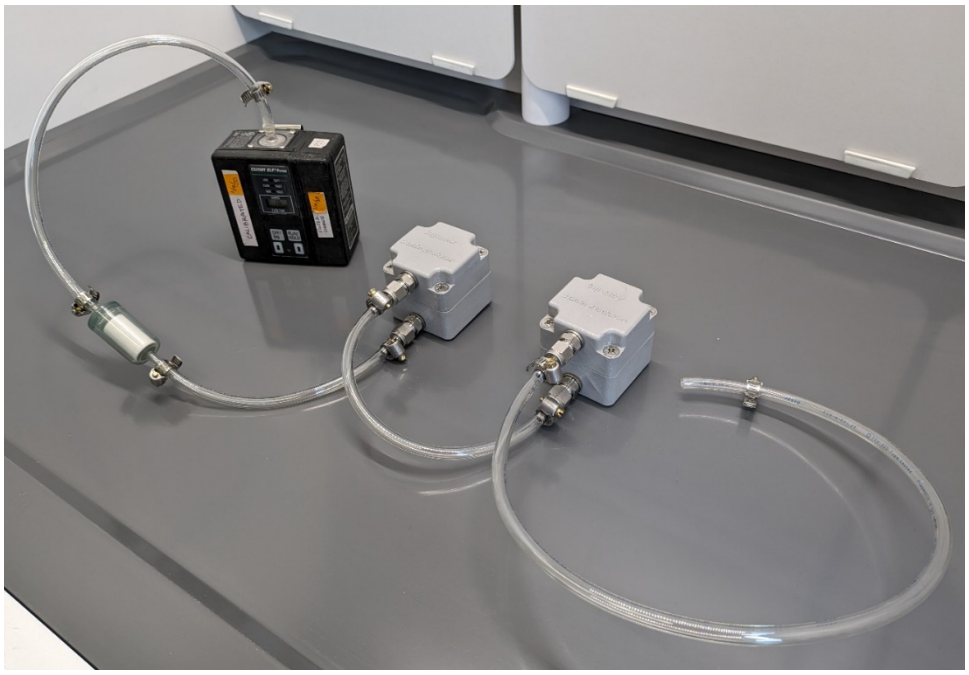

Figure 3.10. AerosolWorks LLC Impactor System.

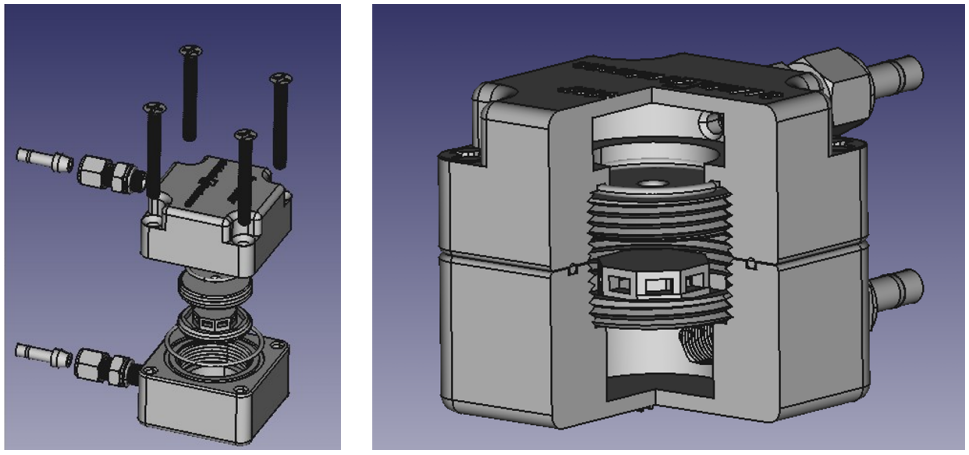

Figure 3.11. Impactor System Design.

3.4.2 Particle size characterization of bulk materials

While an impactor sampling system would ideally enable custom "cut" size(s), the actual distribution of particles is greatly influenced by both the cut sharpness and the distribution of the feed particles (i.e., based on the source material from which dust is being generated). No impactor (and indeed no size selector) can make a perfect cut in particle size, meaning some fraction of particles larger than the cut size will bypass the plate and some fraction of the finer particles will deposit on it; and dust source materials with skewed size distributions might still produce skewed sample distributions. Thus, it is important to characterize the particle size distributions for the source materials to provide some context for interpreting results.

Figure 3.12 shows the particle size distributions for the clean coal, silica, kaolinite, rock dust materials used for this project (i.e., the same materials shown in Table 3.1); these results were obtained using a MicroTrac S3500. The results indicate that most of the particles are smaller than 10 µm for all material types. The implication is that, even though the first impactor should cut at 40 µm and the second should cut at 10 µm, there are just so many fine particles that they will still represent a large fraction of the dust on either impactor stage.

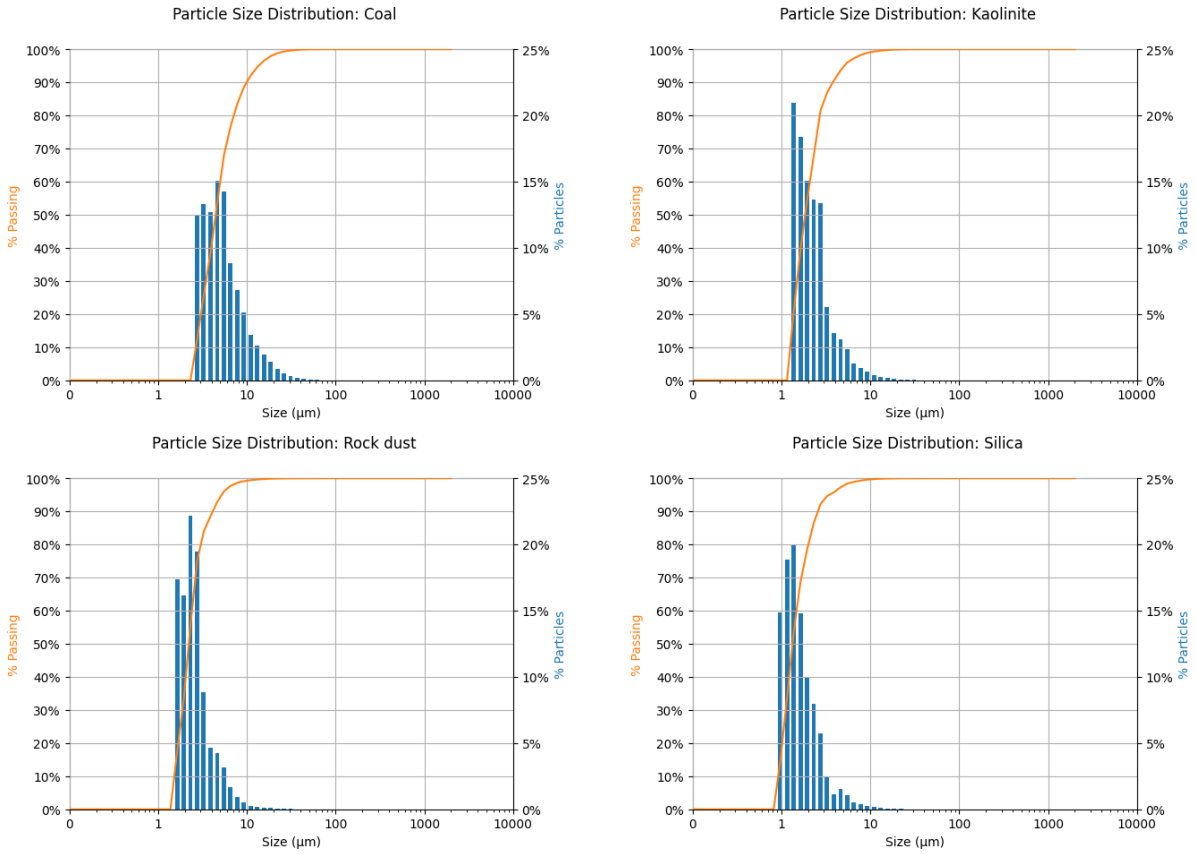

Figure 3.12. MicroTrac particle size distribution results for the four materials used to generate dust samples with larger-than-respirable particles.

3.4.3 Sample collection and Imaging

Using the impactor sampling system, particles from each source material were collected on several slides mounted in the first and second impactor stages. While particles on the first stage slide were somewhat larger than those on the second slide, as expected, both stages had considerable fine particles (i.e., <10 µm) due to the size distribution of the source materials. To maximize the total number of each particle type that could be used to explore optical features, we decided to use both the first and second slide sample for this work.

Table 3.4 shows the summary of image frames captured for each impactor stage and the corresponding number of particles detected for each material type. (It is noted that, due to time constraints, these samples only included particles from a single material). Figure 3.4 shows

the particle size distributions for each material based on the optical microscope imaging. The results are consistent with the particle size distribution obtained from the MicroTrac analysis.

Table 3.4. Dust image inventory for exploring larger-than-respirable particles.

Material	Stage 1 (40µm impactor)	Stage 2 (10µm impactor)	Particles
Coal	123	113	43340
Kaolinite	104	126	10417
Rock dust	33	109	10690
Silica	127	125	22822
Total	**387**	**473**	**87269**

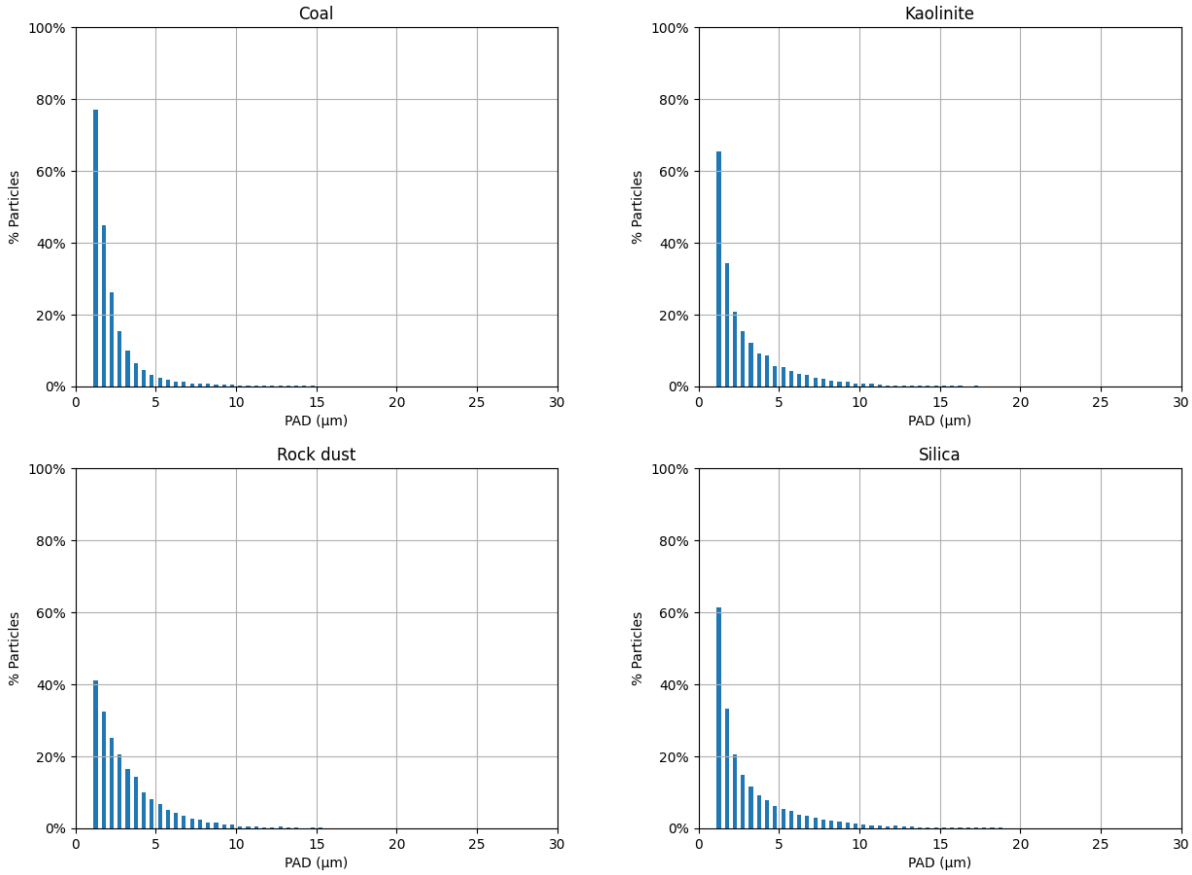

Figure 3.13. Particle size distribution determined from optical images of coal, kaolinite, rock dust, and silica particles collected with the impactor system.

3.4.4 Feature Analysis

Figure 3.14 displays the influence of particle size (PAD) on both AMPI and MMPI metrics. The results show that as the minimum PAD increases, the separation between coal, silicates, and carbonates increases—which indicates that coal/silicates/carbonates model could be improved. On the other hand, when just considering MMPI for mineral separation, there is no clear separation observed for the two silicates (i.e., silica and kaolinite) up to about 15 µm. While

some degree of separation appears to take place with PAD >15 µm, it must be noted that there are very few data points in this range (Figure 3.15). Again, this is attributed to the original size distribution of the source materials.

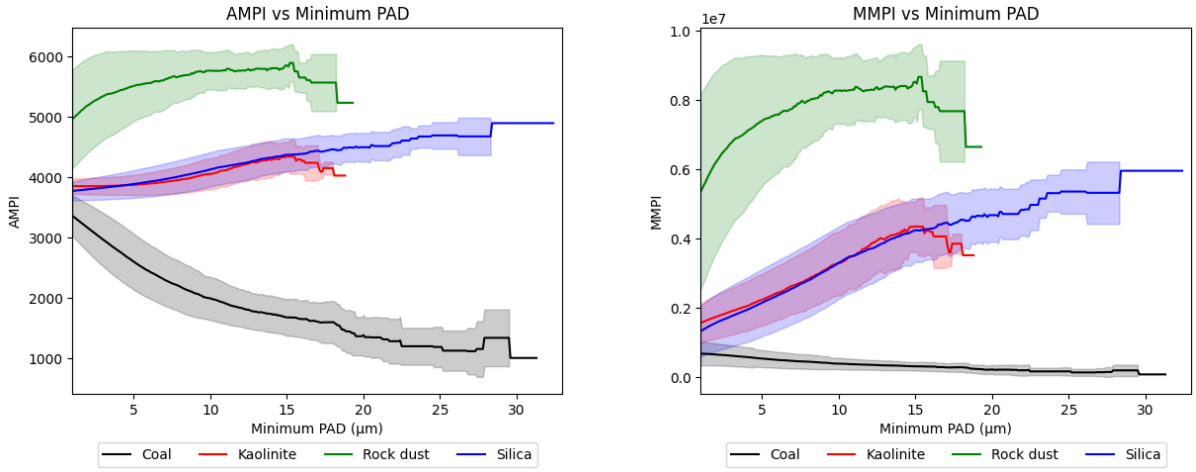

Figure 3.14. Effect of increasing minimum particle size on particle identification.

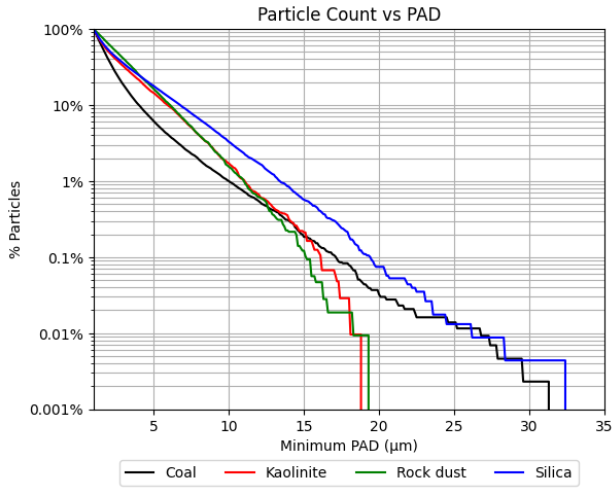

Figure 3.15. Percentage of particles included in the analysis for each particle type given a minimum PAD.

Additional color and texture features were also explored to gauge whether subclassification of silicates may be feasible. These included the mean particle intensities for the red, green, and blue channels in both transmitted PP (TPP) and transmitted CP (TCP) lighting conditions. Moreover, the Gray-Level Co-Occurrence Matrix (GLCM) was considered to evaluate texture features. The GLCM is a statistical method that considers the spatial relationship of pixels in a grayscale image; it was used to assess features such as contrast, correlation, uniformity (sometimes called “energy”), and homogeneity. The results are shown in Figure 3.15. While separation between silica and kaolinite is still not complete for any of the additional features, there is some visible separation between the two particle types under the TPP lighting conditions (both combined and in the RGB channels) and based on the uniformity feature.

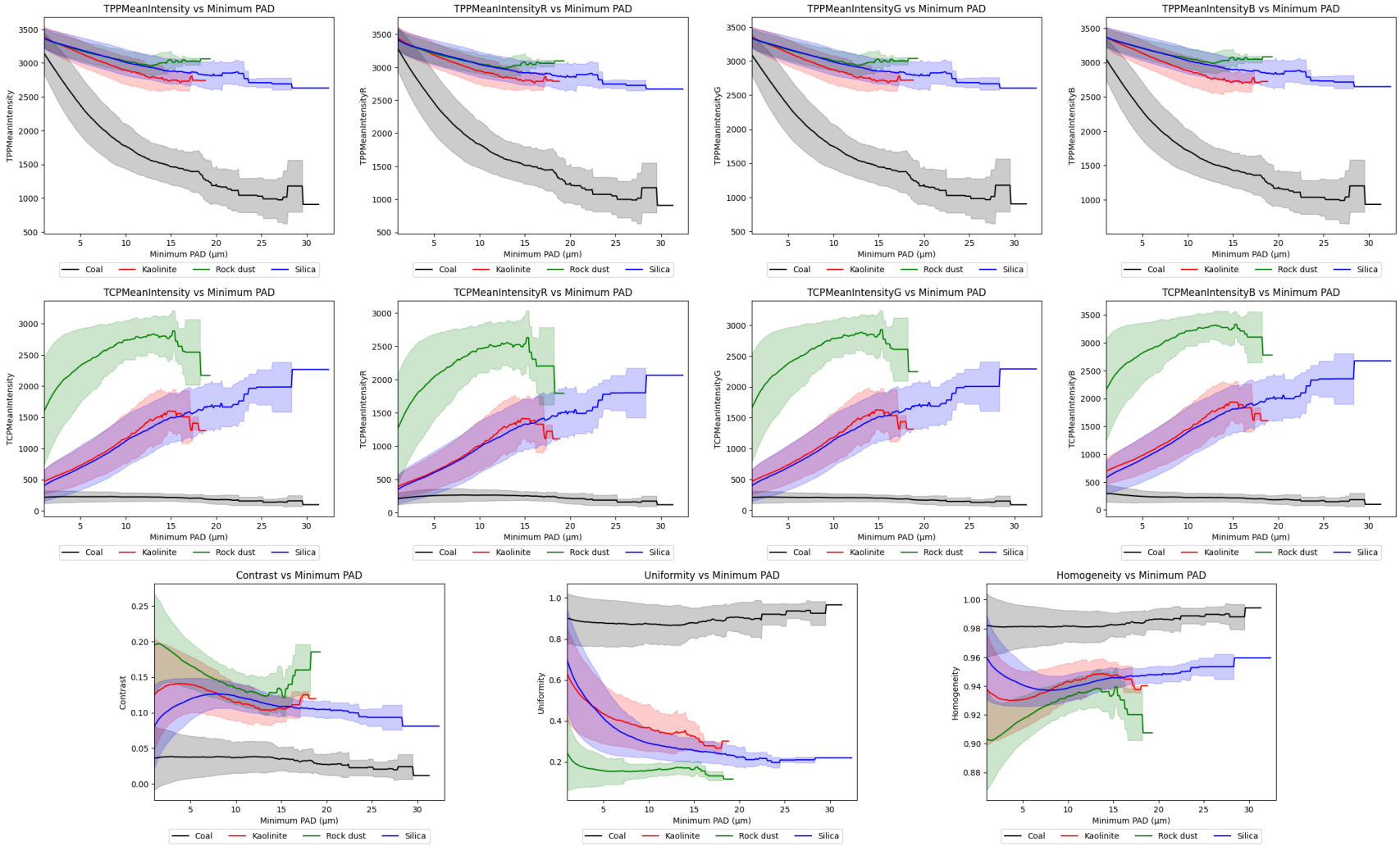

Figure 3.16. Color and texture metrics as a function of particle size (PAD).

3.4.5 Feature Interaction

Based on the above results for each individual feature, we decided to explore whether interactions between the features have any additional potential for silica classification. Interactions between every pair of features in the dataset were analyzed using five different operations: addition, subtraction, multiplication, division, and exponentiation. A total of 678 interaction variables were obtained after filter the data for any undefined values (e.g., such as resulting from division by zero or numbers beyond practical limits).

Analysis of the results indicated that only the interaction of intensity features with texture features such as uniformity yielded separation between silica and kaolinite (see Figure A1 in the Appendix). Separation was most evident when the particle TPP intensity values (mean for all color channels, or for individual RGB channels) were divided by uniformity values. Figure 3.17 shows the results for the mean TPP intensity divided by uniformity as a function of PAD. Even for a minimum PAD of about 10 µm, the plot shows that silica and kaolinite might be separated.

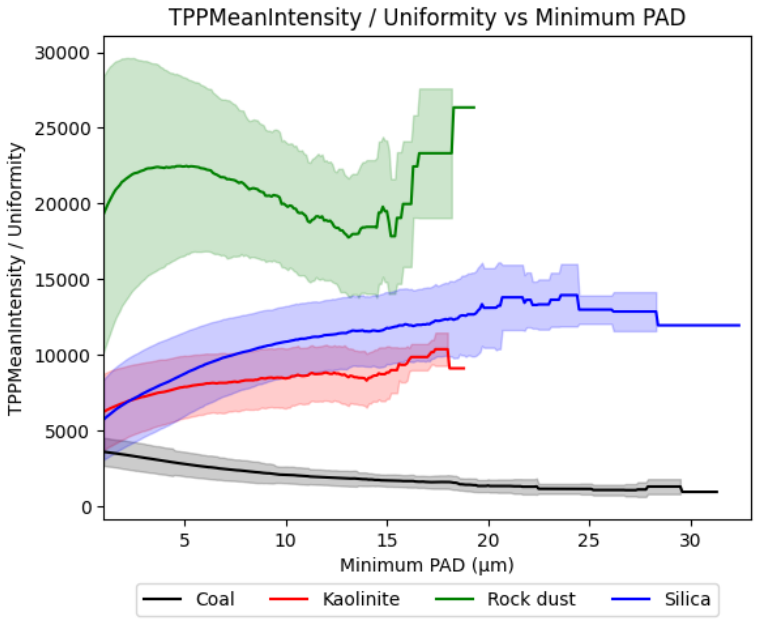

Figure 3.17. Interaction between mean grayscale intensity and uniformity revealing slightly better separation between silica and kaolinite particles as PAD increases.

4 Research Findings and Accomplishments

The work on this project resulted in three main accomplishments as discussed below.

Respirable coal mine dust source apportionment model. In the respirable size range, a model has been developed for classification of particles (as coal, silicate, or carbonate) based only on their optical intensity in TPP and TCP image pairs. Envisioning a portable microscopy application where dust is deposited and imaged frequently, the model could enable a real-time monitor for coal mine dust source apportionment in many operations. This is because the three dust

components that can be classified are often associated with the three primary dust sources in mines: coal, the rock strata surrounding the coal, and rock dust products which are applied to mitigate explosibility hazards.

Identification of optical particle features with potential for silica classification. While a simple method for silica classification using portable microscopy appears unlikely in the respirable size range, results for somewhat larger particles appear promising. Specifically, we found that a combination of light intensity and texture features might be used to separate silica from other silicates if particles are in the 10-20 μm range—which might still be representative of respirable dust in terms of composition.

Development of a sequential sampling and imaging method with particle tracking. To enable direct identification of individual particles based on known dust sources, we devised an innovative method involving sequential sampling (dust deposition) and imaging events, with particle tracking between events. This improved the experimental approach used to develop classification models by removing the need reference measurements using alternative methods that might introduce uncertainty. The general approach devised here could be used or adapted for other applications in the future.

5 Publication Record and Dissemination Efforts

To date, three conference presentations related to this project have been made and one more has been accepted.

1. Santa, N., Keles, C., Saylor, J., & Sarver, E. (Dec 9, 2021) Optical Light Microscopy: A Novel Tool for Near Real Time Coal Mine Dust Monitoring. In 2021 International Future Mining Conference. Online.
2. Santa, N., Keles, C., Saylor, J., & Sarver, E. (Mar 1, 2022). Silica Classification in Respirable Coal Mine Dust Using Optical Microscopy and Image Processing. In 2022 SME Annual Conference and Expo. Salt Lake City, UT.
3. Santa, N., Keles, C., & Sarver, E. (Feb 27, 2023). Refining Respirable Size Silica Particle Identification and Subclassification for Semi-continuous Monitoring Applications. In 2023 SME Annual Conference and Expo. Denver, CO.
4. Santa, N, Sarver, E. (Feb, 2024). Optical Microscopy as the Basis for a Coal Mine Dust Monitor for Simple Source Apportionment. In 2024 SME Annual Conference and Expo. Phoenix, AZ.

Moreover, one journal paper has been submitted for peer review and another is in draft:

5. Santa, N., Sarver, E. (n.d.) Optical Microscopy as a Novel Tool for Respirable Coal Mine Dust Source Apportionment, Coal Science and Technology (submitted).
6. Santa, N., Sarver, E. (n.d.) Effect of Particle Size and Loading Density on Coal Mine Dust Classification by Polarized Light Microscopy (in draft).

6 Conclusions and Impact Assessment

We envision a semi-continuous monitor that uses optical microscopy and image processing to classify coal mine dust. While prior work showed that a binary classification between coal and minerals was possible, on the current project we sought to explore potential for mineral subclassification. In the respirable range, results with lab generated dust from real coal mine materials suggest that minerals can be separated into silicates and carbonates, such that a simple coal/silicates/carbonates classification scheme could support dust source apportionment in some mines. Having this capability in real-time could support a better understanding of trends with changing mining conditions or dust controls. And, in mines where correlations can be established and periodically validated, tracking the silicates component of respirable coal mine dust could serve as a proxy for silica – especially if periodic validation can be performed via conventional sampling and post-hoc laboratory analysis.

Here, work with particles that are somewhat larger than respirable also suggested that silica classification, specifically, could be possible. This is very exciting because—despite the fact that real-time silica monitoring is a top priority in the occupational health and safety field—few analytical methods have shown promise as the basis for a practical devise. However, we acknowledge that the current work is quite preliminary since the samples were all generated in the laboratory from a limited number of source materials.

7 Recommendations for Future Work

Future work to support the envisioned concept for a coal mine dust monitor should include:

- More work on 10-20 µm particles to validate the silica classification results. New work in this area should use dust generated from additional source materials, and it is also necessary to experiment with composite samples.
- Translating the lab-based research to build and test a field prototype. This should include all necessary components for sampling and dust deposition (e.g., size selector, pump, sample substrate), microscopic imaging (lenses, polarizer and analyzer, camera), and image processing (processor). Further, it should consider options for achieving a semi-continuous operation (i.e., how can the sample substrate be cleared or replace in between sampling and imaging events?)

8 References

[1] A. S. Laney and M. D. Attfield, “Coal workers’ pneumoconiosis and progressive massive fibrosis are increasingly more prevalent among workers in small underground coal mines in the United States,” *Occup. Environ. Med.*, vol. 67, no. 6, pp. 428 LP – 431, Jun. 2010, doi: 10.1136/oem.2009.050757.

[2] N. B. Hall, D. J. Blackley, C. N. Halldin, and A. S. Laney, “Current Review of Pneumoconiosis Among US Coal Miners,” *Curr. Environ. Heal. Reports*, 2019, doi: 10.1007/s40572-019-00246-4.

[3] K. S. Almberg *et al.*, “Increased odds of mortality from non-malignant respiratory disease and lung cancer are highest among US coal miners born after 1939,” *Occup. Environ. Med.*, vol. 80, no. 3, pp. 121–128, 2023, doi: 10.1136/oemed-2022-108539.

[4] of Sciences Engineering and Medicine, *Monitoring and Sampling Approaches to Assess Underground Coal Mine Dust Exposures*. Washington, DC: The National Academies Press, 2018.

[5] J. M. Listak, G. J. Chekan, J. F. Colinet, and J. P. Rider, “Performance of a light scattering dust monitor at various air velocities: results of sampling in the active versus the passive mode.,” *International Journal of Miner Res Eng*. pp. 35–47, 2007, [Online]. Available: https://stacks.cdc.gov/view/cdc/9818.

[6] N. Santa, C. Keles, J. R. Saylor, and E. Sarver, “Demonstration of Optical Microscopy and Image Processing to Classify Respirable Coal Mine Dust Particles,” *Minerals*, vol. 11, p. 8, 2021, doi: 10.3390/min11080838.

[7] E. Agioutanti, C. Keles, and E. Sarver, “A thermogravimetric analysis application to determine coal, carbonate, and non-carbonate minerals mass fractions in respirable mine dust,” *J. Occup. Environ. Hyg.*, vol. 17, no. 2–3, pp. 47–58, 2020, doi: 10.1080/15459624.2019.1695057.

[8] L. Jaramillo, E. Agioutanti, S. Ghaychi Afrouz, C. Keles, and E. Sarver, “Thermogravimetric analysis of respirable coal mine dust for simple source apportionment,” *J. Occup. Environ. Hyg.*, vol. 19, no. 9, pp. 568–579, Sep. 2022, doi: 10.1080/15459624.2022.2100409.

[9] E. Sarver, Ç. Keleş, and S. G. Afrouz, “Particle size and mineralogy distributions in respirable dust samples from 25 US underground coal mines,” *Int. J. Coal Geol.*, vol. 247, 2021, doi: 10.1016/j.coal.2021.103851.

[10] C. Keles, N. Pokhrel, and E. Sarver, “A Study of Respirable Silica in Underground Coal Mines: Sources,” *Minerals*, vol. 12, no. 9, 2022, doi: 10.3390/min12091115.

[11] E. Sarver, C. Keles, and M. Rezaee, “Beyond conventional metrics: Comprehensive characterization of respirable coal mine dust,” *Int. J. Coal Geol.*, vol. 207, pp. 84–95, 2019, doi: https://doi.org/10.1016/j.coal.2019.03.015.

[12] F. Animah, A. Greth, C. Keles, and E. Sarver, “Effect of auxiliary scrubbers on respirable coal mine dust particle size and composition,” in *Underground Ventilation*, CRC Press, 2023, pp. 221–229.

[13] F. J. Romay and E. García-Ruiz, “Design of Round-Nozzle Inertial Impactors Review with Updated Design Parameters,” *Aerosol Air Qual. Res.*, vol. 23, no. 3, p. 220436, 2023, doi: 10.4209/aaqr.220436.

Appendix

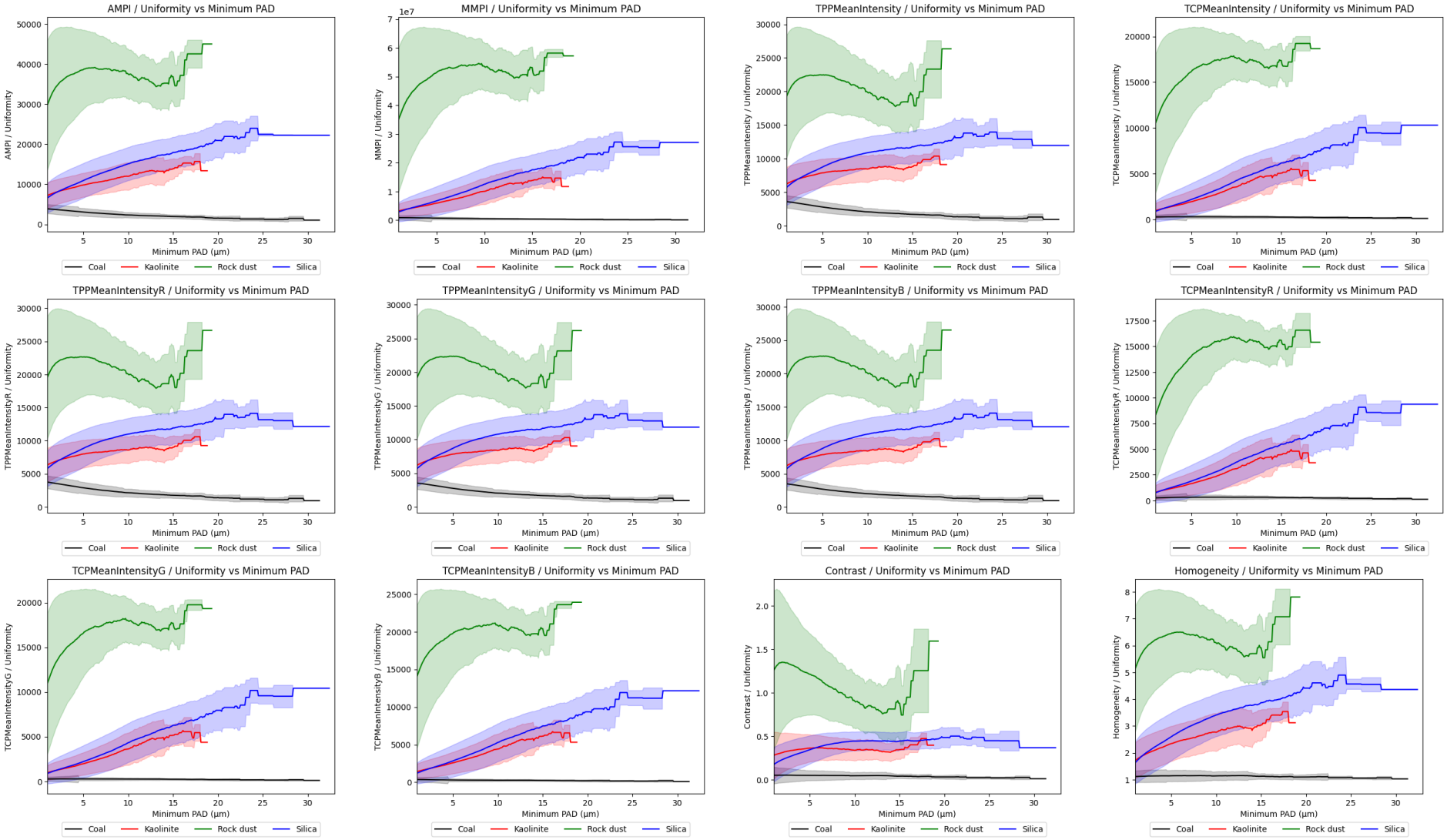

Figure A1. Color or texture metrics divided by uniformity as a function of particle size (PAD).